Progress In Electromagnetics Research C, Vol. 41, 121–135, 2013

BANDWIDTH IMPROVEMENT OF A COMPACT QUADRATURE HYBRID COUPLER WITH HARMONIC REJECTION USING LUMPED ELEMENTS

Yu Ye[1, 2, *], Ling-Yun Li[1], Jian-Zhong Gu[1], and Xiao-Wei Sun[1]

[1]Key Laboratory of Terahertz Solid-State Technology, Shanghai Institute of Microsystem and Information Technology, Shanghai 200050, China

[2]University of Chinese Academy of Sciences, Beijing 100049, China

Abstract—A compact quadrature hybrid coupler with harmonic suppression using lumped-element band-stop resonator is proposed for bandwidth improvement. Conventionally, harmonic rejection is realized by three band-stop resonators in lumped hybrids. The using of three band-stop resonators realizes better harmonic suppression while exhibiting narrower frequency response. So as to improve operation bandwidth behavior, the number of band-stop resonator applied in the proposed topology is minimized to one. Trading off with acceptable reduction in harmonic rejection, the proposed hybrid enlarges working bandwidth with fewer numbers of lumped devices. Detailed design and theoretical analysis are presented and the expressions of lumped elements with dependence of rejected frequency are obtained. To validate the analysis, three 2.45 GHz couplers are fabricated on an FR-4 printed circuit board. The experimental results exhibit 27.3%, 26.9% and 23.3% operation bandwidth with better than 16 dB, 17 dB, and 21 dB harmonic suppressions at 4.9 GHz, 6.1 GHz, and 7.35 GHz, respectively. Less than 0.8 dB amplitude imbalance and 2° phase error are achieved for all the three couplers, which are matched well with theoretical analysis.

Received 17 May 2013, Accepted 22 June 2013, Scheduled 27 June 2013

* Corresponding author: Yu Ye (yye@mail.sim.ac.cn).

1. INTRODUCTION

Hybrid 90° couplers are key components to divide or combine signals with a proper phase difference which are widely implemented in radio frequency (RF) devices, such as power amplifiers, mixers, and antenna systems [1–4]. As couplers are generally designed based on the electrical length of a desired fundamental signal, higher order harmonic signals from those nonlinear devices will degrade the quantity of the desired signal. To suppress those unwanted harmonic signals, external low-pass filters are needed [5, 6]. However, such filters increase circuit size and insertion loss. Besides, as RF wireless systems evolve, independently developed standards, such as long-term evolution (LTE), wireless local area network (WLAN) and mobile world wide interoperability for microwave access (m-WiMAX), increase the number of frequency bands and spectrum fragmentation. Hence, quadrature hybrid couplers for such systems need multimode multiband (MMMB) capability to cover a number of functions, which demands couplers of broader operation frequency range.

Recently, several design techniques have been reported for size reduction and harmonic suppression, such as rat-race couplers with defected ground structure (DGS) and micro-strip resonant cells [7–11] and branch-line couplers using slow-wave structure [12–14]. Wireless communication systems usually require smaller device size in order to meet circuit miniaturization and cost reduction. In lower RF range, although reduction techniques such as multilayer architecture have been utilized, couplers mentioned above still remain too large. Besides, couplers with such complicated structures encounter assembling problems. For instance, couplers with DGS need backside ground apertures that result in unwanted backside radiation [9].

Therefore, in terms of application where circuit size reduction is required, lumped-element devices occupy merely small area is highly attractive. Over the past years, several lumped-element couplers have been reported [15–18]. However, their interests are mainly concentrated on the size reduction. Recently, a lumped-element coupler using band-stop resonators to realize harmonic suppression has been reported [19], where three band-stop resonators are used. However, due to introducing of three band-stop resonators, the bandwidth is narrowed. Besides, when the rejection frequency is closer to the operation frequency, the bandwidth would degrade.

In this work, a novel 90° hybrid coupler with low-pass and high-pass lumped-elements supporting MMMB for m-WiMAX (IEEE 802.16e)/WLAN (IEEE 802.11b/g/n) is proposed. Compared with [19], the only adoption of center band-stop resonator improves

bandwidth behavior while maintaining good harmonic rejection. The about 25% bandwidth supports different bands such as 2.3 GHz (IEEE 802.16e), 2.4 GHz (IEEE 802.11b/g/n), and 2.5–2.7 GHz (IEEE 802.16e). Section 2 gives the theoretical analysis of the coupler based on even- and odd-mode theory. Section 3 describes the experimental results. Conclusions are drawn in Section 4.

2. ARCHITECTURE ANALYSIS

The proposed quadrature coupler with harmonic suppression is shown in Fig. 1. The adoption of band-stop resonator (composed by L_r and C_r) at the center of the topology is for harmonic suppression. Unlike [19], in this topology the number of band-stop resonator is reduced to one to improve working bandwidth. Besides, the number of devices employed in this topology is decreased for size and cost reduction. Overall topology of the proposed hybrid is symmetrical to the vertical center plane. The even-odd decomposition method [20] is

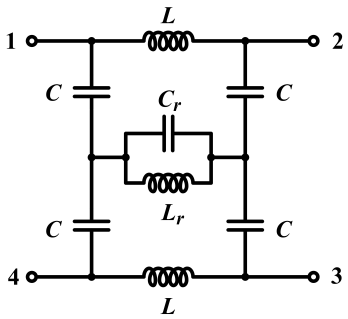

Figure 1. The topology of proposed quadrature hybrid with harmonic suppression using center band-stop resonator.

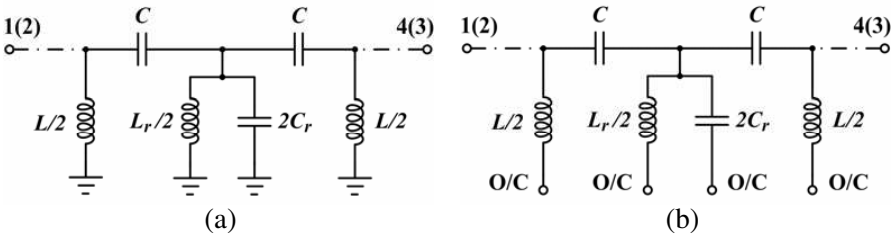

Figure 2. Even- and odd-mode equivalent half circuits of the topology in Fig. 1. (a) Odd mode, (b) even mode.

used for analysis. Figs. 2(a) and (b) depict the odd- and even-mode equivalent half circuits of the topology presented in Fig. 1. The circuits featured in Fig. 2 can be analyzed through the transmission ($ABCD$) matrix method [20].

In the odd-mode circuit, the cross branch are divided in half by the virtual short circuit at the center. The $ABCD$ matrix is expressed by

$$\begin{bmatrix} A & B \\ C & D \end{bmatrix}_{odd} = \begin{bmatrix} 1 & 0 \\ 2/Z_L & 1 \end{bmatrix} \begin{bmatrix} 1 & Z_C \\ 0 & 1 \end{bmatrix} \begin{bmatrix} 1 & 0 \\ 2/Z_R & 1 \end{bmatrix} \begin{bmatrix} 1 & Z_C \\ 0 & 1 \end{bmatrix} \begin{bmatrix} 1 & 0 \\ 2/Z_L & 1 \end{bmatrix}$$

$$= \begin{bmatrix} 1+\frac{2Z_C}{Z_R}+\frac{4Z_C}{Z_L}+\frac{4Z_C^2}{Z_R Z_L} & 2Z_C+\frac{2Z_C^2}{Z_R} \\ \frac{2}{Z_R}+\frac{4}{Z_L}+\frac{8Z_C}{Z_R Z_L}+\frac{8Z_C}{Z_L^2}+\frac{8Z_C^2}{Z_R Z_L^2} & 1+\frac{2Z_C}{Z_R}+\frac{4Z_C}{Z_L}+\frac{4Z_C^2}{Z_R Z_L} \end{bmatrix} \quad (1a)$$

where $Z_R = j\omega L_r/(1-\omega^2 L_r C_r)$, $Z_L = j\omega L$ and $Z_C = 1/j\omega \mathrm{C}$ are the equivalent impedance of the resonator, inductor L and capacitor C, respectively. In the even-mode half circuit, the cross branch can be divided in half by the virtual open circuit (O/C) at the center. The $ABCD$ matrix is expressed as follow:

$$\begin{bmatrix} A & B \\ C & D \end{bmatrix}_{even} = \begin{bmatrix} 1 & 2Z_C \\ 0 & 1 \end{bmatrix} \quad (1b)$$

The relationship of scattering matrix and $ABCD$ matrix is obtained by [21]:

$$[S] = \begin{bmatrix} S_{11} & S_{21} \\ S_{12} & S_{22} \end{bmatrix} = \begin{bmatrix} \frac{A+B/Z_0-CZ_0-D}{\Delta} & \frac{2(AD-BC)}{\Delta} \\ \frac{2}{\Delta} & \frac{-A+B/Z_0-CZ_0+D}{\Delta} \end{bmatrix} \quad (2)$$

where $\Delta = A + B/Z_0 + CZ_0 + D$, and Z_0 is the port impedance in the system. As a reciprocal symmetrical network, $S_{ik} = S_{ki}$ and $\det[ABCD] = 1$ can be identified [22]. So

$$AD - BC = 1 \quad (3)$$

The scattering matrices of the odd- and even-mode are illustrated as

$$[S]_{odd} = \frac{2}{\Delta_{odd}} \begin{bmatrix} S'_{11} & 1 \\ 1 & S'_{22} \end{bmatrix} \quad (4a)$$

$$[S]_{even} = \frac{2}{\Delta_{even}} \begin{bmatrix} Z_C/Z_0 & 1 \\ 1 & Z_C/Z_0 \end{bmatrix} \quad (4b)$$

where S'_{11}, S'_{22}, Δ_{odd} and Δ_{even} are written as:

$$S'_{11} = S'_{22} = \frac{Z_C}{Z_0} + \frac{Z_C^2}{Z_R Z_0} - \frac{Z_0}{Z_R} - \frac{2Z_0}{Z_L} - \frac{4Z_C Z_0}{Z_R Z_L} - \frac{4Z_C Z_0}{Z_L^2} - \frac{4Z_C^2 Z_0}{Z_R Z_L^2} \quad (5a)$$

$$\Delta_{odd} = 2 + \frac{2Z_C}{Z_0} + 4\left(\frac{Z_C}{Z_R} + \frac{2Z_C}{Z_L} + \frac{2Z_C^2}{Z_R Z_L}\right) + 2\left(\frac{Z_C^2}{Z_0 Z_R} + \frac{2Z_0}{Z_L} + \frac{Z_0}{Z_R} + \frac{4Z_0 Z_C}{Z_R Z_L} + \frac{4Z_0 Z_C}{Z_L^2} + \frac{4Z_0 Z_C^2}{Z_R Z_L^2}\right) \quad (5b)$$

$$\Delta_{even} = 2 + \frac{2Z_C}{Z_0} \quad (5c)$$

The scattering parameters (S-parameters) of the hybrid are given by

$$S_{11} = \frac{1}{2}\left(S_{11}^e + S_{11}^o\right) \quad (6a)$$

$$S_{21} = \frac{1}{2}\left(S_{11}^e - S_{11}^o\right) \quad (6b)$$

$$S_{31} = \frac{1}{2}\left(S_{21}^e - S_{21}^o\right) \quad (6c)$$

$$S_{41} = \frac{1}{2}\left(S_{21}^e + S_{21}^o\right) \quad (6d)$$

At the operation frequency ω_0, with (3), the following equation is obtained:

$$4\left(\frac{Z_C}{Z_R}\right)\left(\frac{Z_C}{Z_R} + 1\right)\left(\frac{2Z_C}{Z_L} + 1\right)\left(\frac{2Z_R}{Z_L} + \frac{2Z_C}{Z_L} + 1\right) = 0 \quad (7)$$

To satisfy (7), the ratio of (Z_C/Z_R) equals to -1, which is a unique solution at the frequency ω_0. Besides, if the band-stop resonator's resonant frequency is defined to be ω_r, the relationship between ω_r and ω_0 can be obtained as $\omega_r^2 = 1/L_r C_r = (k\omega_0)^2$, where k is the ratio of (ω_r/ω_0). When the conditions of $L = Z_0/\omega_0$ and $C = 1/(\omega_0 Z_0)$ are set [15], $S_{11} = S_{41} = 0$ is proven at the frequency ω_0. L, L_r, C, and C_r are:

$$L = \frac{Z_0}{\omega_0} \quad (8a)$$

$$L_r = \left(1 - \frac{1}{k^2}\right)\frac{Z_0}{\omega_0} \quad (8b)$$

$$C = \frac{1}{\omega_0 Z_0} \quad (8c)$$

$$C_r = \frac{1}{(k^2 - 1)\,\omega_0 Z_0} \quad (8d)$$

Thus, the Equations 6(b) and (c) are

$$S_{21} = \frac{1}{2}(1-j) \tag{9a}$$

$$S_{31} = \frac{1}{2}(1+j) \tag{9b}$$

From the above expressions, it is evident that at the center frequency ω_0 the hybrid is matched and has perfect isolation. The power that exited at port 1 is delivered identically to ports 2 and 3 with a quadrature phase difference. The theoretical hybrid scattering matrix at the frequency ω_0 is obtained by

$$[S]_{coupler} = \frac{1}{2}\begin{bmatrix} 0 & 1-j & 1+j & 0 \\ 1-j & 0 & 0 & 1+j \\ 1+j & 0 & 0 & 1-j \\ 0 & 1+j & 1-j & 0 \end{bmatrix} \tag{10}$$

The relationship of unwanted harmonic frequency and ω_0 can be defined as $\omega_h = n\omega_0$, where ω_h is the unwanted harmonic frequency and n the rejected harmonic index. For perfect power rejection at frequency $n\omega_0$, the transmission coefficients from port 1 to ports 2 and 3 need to be zero, which is written as follow

$$S_{21} = S_{31} = 0 \tag{11}$$

Substitute S_{21} and S_{31} by (6b) and (6c), $\Delta_{odd} = \Delta_{even}$ is derived at frequency $n\omega_0$ to satisfy (11). Then the following equation is derived as

$$4\left(\frac{Z_C}{Z_R} + \frac{2Z_C}{Z_L} + \frac{2Z_C^2}{Z_R Z_L}\right) + 2\left(\frac{Z_C^2}{Z_0 Z_R} + \frac{2Z_0}{Z_L} + \frac{Z_0}{Z_R} + \frac{4Z_0 Z_C}{Z_R Z_L} + \frac{4Z_0 Z_C}{Z_L^2} + \frac{4Z_0 Z_C^2}{Z_R Z_L^2}\right) = 0 \tag{12}$$

An approximate equation based on (12) can be expressed as

$$4jk + 8jk\left(\frac{n^2-1}{n^2-k^2}\right) - 8j\frac{1}{k} = 0 \tag{13}$$

The solution to (12) is

$$k^2 = \frac{n^4}{3n^2-2} \tag{14}$$

then L_r and C_r can be written as

$$L_r = \left(1 - \frac{3n^2-2}{n^4}\right)\frac{Z_0}{\omega_0} \tag{15a}$$

$$C_r = \frac{1}{\left(\frac{n^4}{3n^2-2} - 1\right)\omega_0 Z_0} \tag{15b}$$

So the band-stop resonator used in the proposed topology can be selected using (15a) and (15b) to achieve transmission stop at $n\omega_0$. Thus, S_{21} and S_{31} of the coupler at frequency $n\omega_0$ are given by

$$S_{21} = -S_{31} = \frac{1}{2}\left[\frac{j}{n-j} - \frac{jn}{(n^2-2)-jn}\right] \tag{16}$$

According to (16), the theoretical out-of-band harmonic suppression is plotted in Fig. 3(a). The harmonic rejection performance improves when the harmonic index, n, increases. When n is bigger than 2.3, theoretically the coupler provides over 20 dB harmonic rejection. Over 30 dB harmonic rejection is achieved when n is bigger than 3. Theoretical normalized frequency dependence of the S-parameters for the coupler with $n = 2$, 2.5 and 3, respectively, are shown in Figs. 3(b), (c) and (d). When $n = 2$, 2.5 and 3, the coupler exhibits theoretical operation bandwidth of 25.3% (0.971–1.224), 26.5% (0.959–1.224), and 24.9% (0.943–1.192), respectively. Less than 4 dB insertion loss (IL) and better than 10 dB, 13 dB and 15 dB return loss are achieved within the operation bandwidth, respectively, for $n = 2$, 2.5 and 3. The amplitude imbalance (AI) and phase difference (PD) between ports 2 and 3 are illustrated in Figs. 3(e) and (f). Less than 1 dB AI and less than 5° PD are achieved with $n = 2$, 2.5 and 3, while the harmonic rejection are better than 16 dB, 22 dB and 27 dB, respectively. As shown in Fig. 3, in contrast to [19], the AI and PD of the proposed couplers are improved. Besides, the below −20 dB return loss and isolation of the proposed couplers remain similar with [19]. However, at the upper side operation band, the performance degrades if the rejected harmonic frequency is close to the operational frequency. As tabulated in Table 1, although not as good as [19] in rejection behavior, the proposed topology provides wider operation bandwidth while with acceptable harmonic rejection. Besides, the fewer number of lumped devices reduce the size and cost.

3. IMPLEMENTATION OF LUMPED-ELEMENT QUADRATURE COUPLER

A low-cost FR-4 printed circuit board with a dielectric constant of 4.5 and thickness of 0.8 mm was employed to validate analytical results, where the surface mounted devices (SMD) of the lumped inductors and capacitors are adopted. Three lumped quadrature couplers with $n = 2$, 2.5 and 3 were fabricated. The values of the passive lumped elements L, L_r, C, and C_r are 3.3 nH/1.2 nH/1.3 pF/2.2 pF, 3.3 nH/1.9 nH/1.3 pF/1 pF, and 3.3 nH/2.3 nH/1.3 pF/0.6 pF for $n = 2$, 2.5 and 3, respectively. The couplers with harmonic suppression are

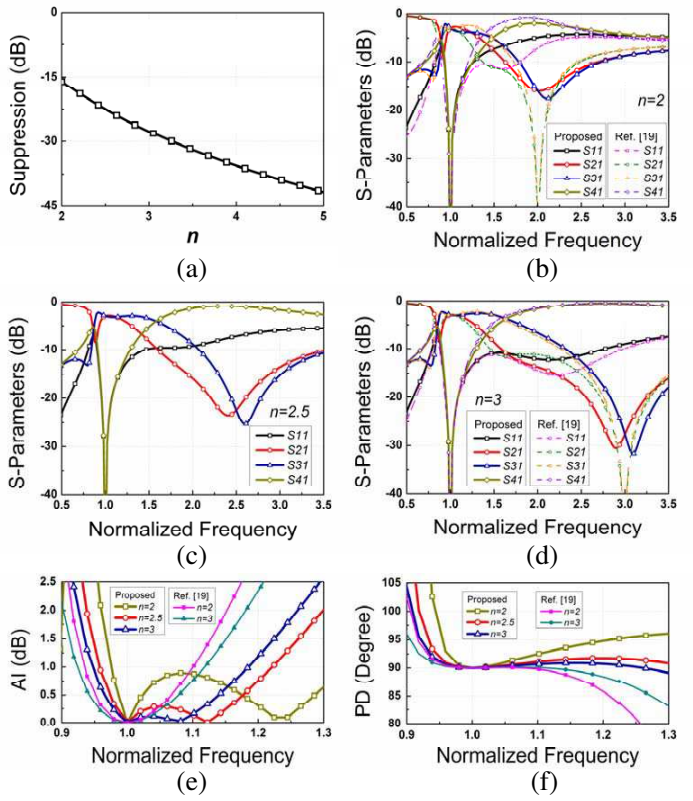

Figure 3. Theoretical analysis results in contrast with [19]. (a) Harmonic suppression tuned with n. (b) S-parameters when $n = 2$. (c) S-parameters when $n = 2.5$. (d) S-parameters when $n = 3$. (e) AI with different n (2, 2.5 and 3). (f) PD with different n (2, 2.5 and 3).

implemented at 2.45 GHz. Photographs of the fabricated circuits are featured in Fig. 4. The overall dimension of the core circuit is only 2 mm × 2.2 mm for each hybrid coupler. An Agilent PNA N5245A four-port network analyzer was used to obtain measurements of the couplers.

The measured results and theoretical simulated results of S-parameters for $n = 2$, 2.5 and 3 are demonstrated in Fig. 5, where measured results are in good agreement with theoretical analysis. The measured performance of AI and PD between the direct port and the coupled port are illustrated in Fig. 6 with different harmonic rejection ($n = 2$, 2.5 and 3). The measured IL with different n are also plotted in Fig. 6.

Table 1. Theoretical performance comparison between this work and [19].

	This work		[19]	
n	Bandwidth*	Harmonic Rejection	Bandwidth*	Harmonic Rejection
2	25.3%	> 16 dB	16.5%	> 30 dB
2.5	26.5%	> 22 dB	18.3%	> 30 dB
3	24.9%	> 27 dB	19.5%	> 30 dB

*Bandwidth: Return loss/Isolation > 10 dB, IL < 4 dB, amplitude imbalance < 1 dB and phase error < 5 degrees.

When $n = 2$, the coupler has a 27.3% operation bandwidth ranging from 2.4 GHz to 3.06 GHz. As shown in Fig. 6(b), within the operation bandwidth the IL is 3.8 ± 0.4 dB, while a better than 12 dB return loss and a better than 10 dB isolation are observed. At the center frequency of 2.45 GHz, the measured return loss and isolation are 22 dB and 19 dB, respectively. As featured in Fig. 6(a), the measured AI between the direct port and the coupled port is less than 0.5 dB with a $90° \pm 2°$ PD. Furthermore, as illustrated in Fig. 5(a), the coupler exhibits a 16 dB second harmonic suppression at 4.9 GHz. The better than 14 dB rejection is from 4.7 GHz to 5.2 GHz.

When $n = 2.5$, the coupler possesses a 26.9% operation bandwidth ranging from 2.3 GHz to 2.95 GHz. As indicated in Fig. 6(d), within the bandwidth the IL is 3.7 ± 0.5 dB, while a better than 15 dB return loss and a better than 14 dB isolation are obtained. At the center frequency, the measured return loss and isolation are 25 dB and 23 dB, respectively. As featured in Fig. 6(c), the measured AI between the direct port and the coupled port is less than 0.6 dB with a $90° \pm 2°$

(a) (b) (c)

Figure 4. Photograph of the fabricated couplers with different rejected harmonic frequency. (a) $n = 2$. (b) $n = 2.5$. (c) $n = 3$.

PD. Besides, as illustrated in Fig. 5(b), the coupler exhibit 16 dB and 17 dB harmonic suppression in the direct port and the coupled port at 6.1 GHz, respectively. The better than 15 dB rejection is from 5.3 GHz to 6.3 GHz.

When $n = 3$, the coupler exhibits a 24.1% operation bandwidth from 2.28 GHz to 2.86 GHz. As featured in Fig. 6(f), the IL is 3.7 ± 0.4 dB, while a better than 15 dB return loss and a better than 14 dB isolation are achieved. The measured return loss and isolation are 29 dB and 22 dB at 2.45 GHz, respectively. The measured AI between the direct port and the coupled port is less than 0.8 dB with a $90° \pm 2°$ PD, which are featured in Fig. 6(e). Furthermore, as illustrated in Fig. 5(c), the coupler exhibits 30 dB and 21 dB third harmonic suppressions in the direct port and the coupled port at 7.3 GHz, respectively. The better than 15 dB rejection is from 6.3 GHz to 8.4 GHz.

These measured results illustrate that the proposed coupler achieves good operation performance with sufficient out-band rejection. Furthermore, the measured results validate the analytical solutions in a good agreement. However, IL degrades when compared to the theoretical analysis, which may because of the parasitic effects and component diversions of the SMDs. For better understanding, a $\pm 5\%$ tolerance in each component is included, which is reasonable in common SMDs. The statistical simulated results of S_{21} and S_{31}

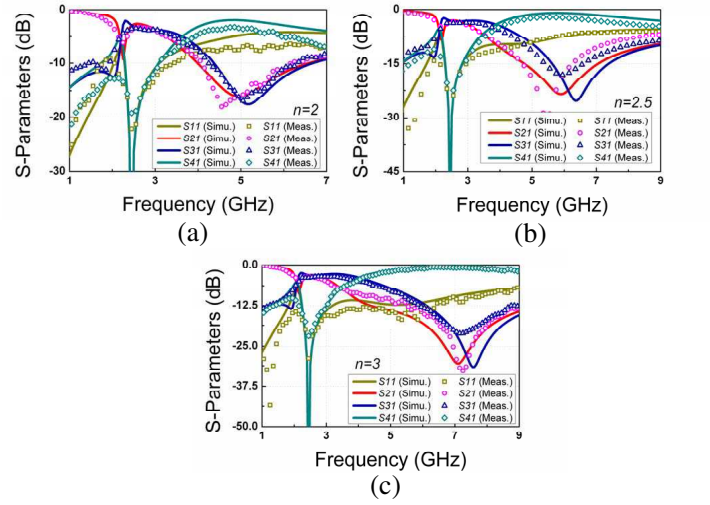

Figure 5. Measured and theoretical simulated results of S-parameters with different n. (a) $n = 2$. (b) $n = 2.5$. (c) $n = 3$.

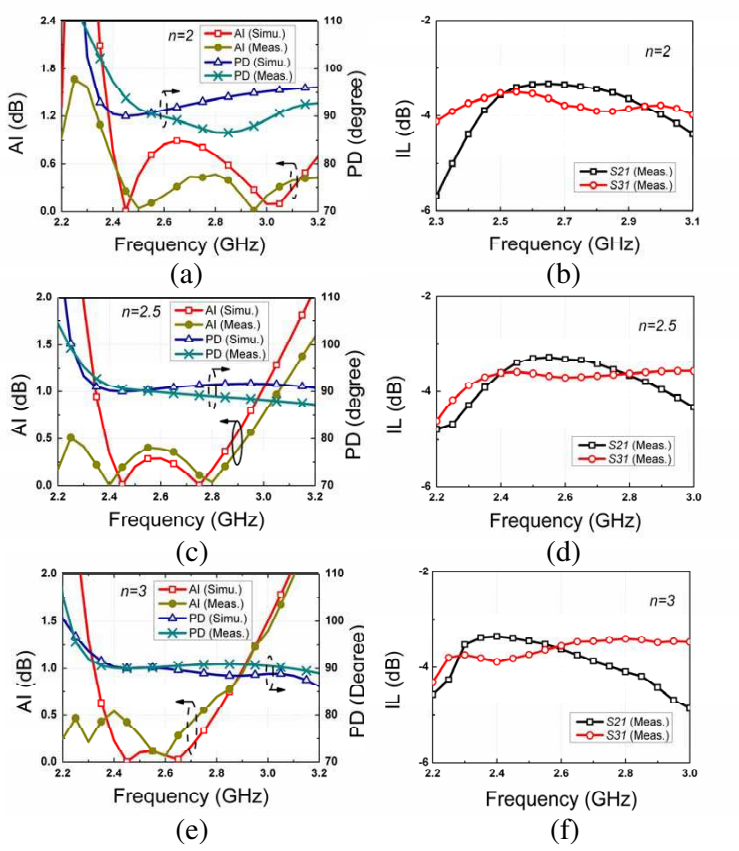

Figure 6. Measured and theoretical simulated results of the AI, PD and IL with different n. (a) AI and PD ($n = 2$). (b) IL ($n = 2$). (c) AI and PD ($n = 2.5$). (d) IL ($n = 2.5$). (e) AI and PD ($n = 3$). (f) IL ($n = 3$).

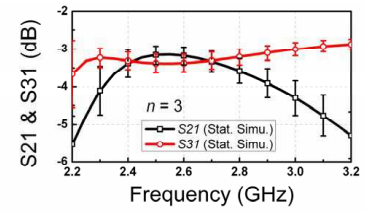

Figure 7. Statistical simulation results of the proposed coupler with $n = 3$, where a $\pm 5\%$ tolerance is included in each component and its parasitic resistance.

Table 2. Performance comparison between this work and published work.

Reference	Frequency (f_0)	Bandwidth	Harmonic Rejection	Size (mm^2)	Tech.
[7]	2 GHz	5%	> 30 dB ($2f_0 - 4f_0$)	13.89×17.62	Rat-race
[8]	2.45 GHz	20.4%	> 20 dB ($3f_0 - 5f_0$)	306.35	Rat-race
[11]	900 MHz	13%	> 20 dB ($2f_0$)	18×34.5	Rat-race
[12]	2 GHz	10%	> 22.5 dB ($2f_0$)	265.69	Branch-line
[13]	836.5 MHz	6%	> 18 dB ($2f_0$)	27.75×25.7	Branch-line
[14]	1 GHz	16%	> 20 dB ($4f_0 - 6f_0$)	30.2×31.7	Branch-line
[19]	2.45 GHz	16.3%	> 25 dB ($2f_0$)	2×2.5	SMD
This Work*	2.45 GHz	27.3%	> 16 dB ($2f_0$)	2×2.2	SMD
This Work*	2.45 GHz	26.9%	> 17 dB ($2.5f_0$)	2×2.2	SMD
This Work*	2.45 GHz	24.1%	> 20 dB ($3f_0$)	2×2.2	SMD

*Bandwidth: Return loss/Isolation > 10 dB, IL < 4 dB, AI < 0.8 dB and phase error < 2 degrees.

are illustrated in Fig. 7, which shows approximate ± 0.3 dB variations in S_{21} and S_{31} around the operation frequency. Considering these statistical variations, the measured results are within an acceptable variation range. It features a reasonable deviation between theoretical and measured results. Table 2 tabulates the comparisons between this work and previous published reports. As listed in Table 2, in contrast with rat-race or branch-line couplers, this compact topology provides harmonic rejection with significant size and cost reduction. What's more, with similar in-band performance such as IL, return loss, and PD, compared to previous reports, this topology exhibits wider operation frequency range.

4. CONCLUSION

A compact quadrature hybrid coupler with harmonic suppression using lumped-element band-stop resonator is presented. In order to improve the operation bandwidth while with sufficient harmonic rejection, in the proposed topology the number of band-stop resonator is minimized to one. Besides, compared to rat-race or branch-line couplers, this topology provides harmonic rejection with significant size and cost reduction. Detailed design and theoretical analysis are presented for the proposed coupler and the expressions of lumped elements are obtained. Promising agreements between experimental results and theoretical analysis are achieved. In contrast to other lumped-element couplers with harmonic rejection, the proposed topology exhibits wider operation frequency which can be applied in MMMB system for m-WiMAX (IEEE 802.16e)/WLAN (IEEE 802.11b/g/n).

ACKNOWLEDGMENT

This work is supported by National Science and Technology Major Project (No. 2011ZX0300400202).

REFERENCES

1. Ozis, D., J. Paramesh, and D. J. Allstot, "Integrated quadrature couplers and their application in image-reject receivers," *IEEE J. Solid-State Circuits.*, Vol. 44, No. 5, 1464–1476, May 2009.
2. Chang, C.-W., Y.-J. E. Chen, and J.-H. Chen, "A power-recycling technique for improving power amplifier efficiency under load mismatch," *IEEE Microw. Wireless Compon. Lett.*, Vol. 21, No. 10, 571–573, Oct. 2011.
3. Bulus, U., O. Kizilbey, H. Aniktar, and A. Gunes, "Broadband direction-finding antenna using suspended microstrip-line hybrid coupler for handheld devices," *IEEE Antennas Wireless Propag. Lett.*, Vol. 12, 80–83, 2013.
4. Shu, P. and Q. Feng, "Design of a compact quad-band hybrid antenna for compass/WiMAX/MLAN applications," *Progress In Electromagnetics Research*, Vol. 138, 585–598, 2013.
5. Wong, Y. S., S. Y. Zheng, and W. S. Chan, "Multifolded bandwidth branch line coupler with filtering characteristic using coupled port feeding," *Progress In Electromagnetics Research*, Vol. 118, 17–35, 2011.

6. Cheng, Y. J., L. Wang, J. Wu, and Y. Fan, "Directional coupler with good restraint outside the passband and its frequency-agile application," *Progress In Electromagnetics Research*, Vol. 135, 759–771, 2013.
7. Wang, W.-H., T.-M. Huang, and R.-B. Wu, "Miniatured rat-race coupler with bandpass response and good stopband rejection," *IEEE MTT-S Int. Microwave Symp. Dig.*, 709–712, 2009.
8. Kuo, J.-T., J.-S. Wu, and Y.-C. Chiou, "Miniaturized rat race coupler with suppression of spurious passband," *IEEE Microw. Wireless Compon. Lett.*, Vol. 17, No. 1, 46–48, Aug. 2007.
9. Sung, Y. J., C. S. Ahn, and Y.-S. Kim, "Size reduction and harmonic suppression of rat-race hybrid coupler using defected ground structure," *IEEE Microw. Wireless Compon. Lett.*, Vol. 14, No. 1, 7–9, Jan. 2004.
10. Gu, J.-Z. and X.-W. Sun, "Miniaturization and harmonic suppression rat-race coupler using C-SCMRC resonators with distributive equivalent circuit," *IEEE Microw. Wireless Compon. Lett.*, Vol. 15, No. 12, 880–882, Dec. 2005.
11. Chiu, H.-C., C.-H. Lai, and T.-G. Ma, "Miniaturized rat-race coupler with out-of-band suppression using double-layer synthesized coplanar waveguides," *IEEE MTT-S Int. Microwave Symp. Dig.*, 2012.
12. Wang, J., B.-Z. Wang, Y.-X. Guo, L. C. Ong, and S. Q. Xiao, "A compact slow-wave microstrip branch-line coupler with high performance," *IEEE Microw. Wireless Compon. Lett.*, Vol. 17, No. 7, 501–503, Jul. 2007.
13. Tsai, K.-Y., H.-S. Yang, J.-H. Chen, and Y.-J. E. Chen, "A miniaturized 3 dB branch-line hybrid coupler with harmonics suppression," *IEEE Microw. Wireless Compon. Lett.*, Vol. 21, No. 10, 537–539, Oct. 2011.
14. Hazeri, A. R. and T. Faraji, "Miniaturization and harmonic suppression of the branch-line hybrid coupler," *Int. J. Electron*, Vol. 98, No. 12, 1699–1710, Dec. 2011.
15. Hou, J. A. and Y. H. Wang, "A compact quadrature hybrid based on high-pass and low-pass lumped elements," *IEEE Microw. Wireless Compon. Lett.*, Vol. 17, No. 8, 595–597, Aug. 2007.
16. Ohta, I., X. P. Li, T. Kawai, and Y. Kokubo, "A design of lumped-element 3 dB quadrature hybrids," *Proc. Asia-Pacific Microw. Conf.*, Vol. 3, 1141–1144, Dec. 1997.
17. Chiang, Y. C. and C. Y. Chen, "Design of a wideband lumped-element 3-dB quadrature coupler," *IEEE Trans. on Microw.*

Theory and Tech., Vol. 49, No. 3, 476–479, 2001.

18. Vogel, R. W., "Analysis and design of lumped and lumped distributed element directional couplers for MIC and MMIC applications," *IEEE Trans. on Microw. Theory and Tech.*, Vol. 40, No. 2, 253–262, 1992.
19. Hou, J. A. and Y. H. Wang, "Design of compact 90° and 180° couplers with harmonic suppression using lumped-element bandstop resonators," *IEEE Trans. on Microw. Theory and Tech.*, Vol. 58, No. 11, 2932–2939, Nov. 2010.
20. Reed, J. and G. J. Wheeler, "A method of analysis of symmetrical four-port networks," *IEEE Trans. on Microw. Theory and Tech.*, Vol. 4, No. 4, 246–252, Oct. 1956.
21. Pozar, D. M., *Microwave Engineering*, Artech House, Norwell, MA, 1990.
22. Faria, J. A., *Multiconductor Transmission-line Structures*, New York, Wiley, 1993.